

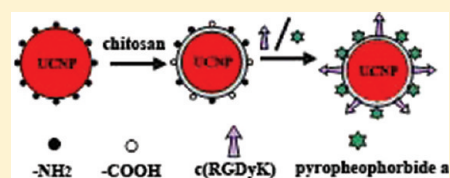
Pyropheophorbide A and c(RGDyK) Comodified Chitosan-Wrapped Upconversion Nanoparticle for Targeted Near-Infrared Photodynamic Therapy

Aiguo Zhou, Yanchun Wei, Baoyan Wu, Qun Chen, and Da Xing*

MOE Key Laboratory of Laser Life Science & Institute of Laser Life Science, College of Biophotonics, South China Normal University, Guangzhou 510631, China

Supporting Information

ABSTRACT: Near-infrared (NIR)-to-visible upconversion nanoparticle (UCNP) has shown promising prospects in photodynamic therapy (PDT) as a drug carrier or energy donor. In this work, a photosensitizer pyropheophorbide a (Ppa) and RGD peptide c(RGDyK) comodified chitosan-wrapped NaYF₄:Yb/Er upconversion nanoparticle UCNP-Ppa-RGD was developed for targeted near-infrared photodynamic therapy. The properties of UCNP-Ppa-RGD, such as morphology, stability, optical spectroscopy and singlet oxygen generation efficiency, were investigated. The results show that covalently linked pyropheophorbide a molecule not only is stable but also retains its spectroscopic and functional properties. In vitro studies confirm a stronger targeting specificity of UCNP-Ppa-RGD to integrin $\alpha_v\beta_3$ -positive U87-MG cells compared with that in the corresponding negative group. The photosensitizer-attached nanostructure exhibited low dark toxicity and high phototoxicity against cancer cells upon 980 nm laser irradiation at an appropriate dosage. These results represent the first demonstration of a highly stable and efficient photosensitizer modified upconversion nanostructure for targeted near-infrared photodynamic therapy of cancer cells. The novel UCNP-Ppa-RGD nanoparticle may provide a powerful alternative for near-infrared photodynamic therapy with an improved tumor targeting specificity.



KEYWORDS: upconversion nanoparticle, chitosan, pyropheophorbide a, c(RGDyK), PDT, 980 nm laser

INTRODUCTION

Photodynamic therapy (PDT) is an emerging cancer treatment modality involving a combination of light, photosensitizer (PS), and molecular oxygen. It offers unique control in the photosensitizer's action, because the key cytotoxic agent, singlet oxygen ($^1\text{O}_2$), is produced only upon in situ irradiation.¹ PDT can be used as a primary therapy for early stage disease, palliation of late stage disease, or as a surgical adjuvant for tumors that show locoregional spread.^{2–5}

Although PDT has been widely used in clinical application, there are still several challenges that should be overcome to enhance its treatment efficiency. The first one is to improve the therapeutical depth of PDT. There is an "optical window" of tissue from 700 to 1100 nm, where tissue has maximum transparency to light. So the therapeutical depth of PDT would be greatly improved if the excitation light lies within this window.⁶ The second one is to improve the selectivity of photosensitizers to tumors. Photosensitizers are known to spontaneously accumulate in tumors with leaky vasculature by an enhanced permeability and retention (EPR) effect.^{7–9} However, most anticancer drugs are not selective enough due to their accumulation in normal tissues. Selectivity can be further enhanced by combining the photosensitizer with molecular delivery systems or by conjugating it with targeting agents such as monoclonal antibodies, receptor ligands or recognition peptides.¹⁰ Another challenge to PDT is the

process of photosensitizer delivery. Since most commonly used photosensitizers are hydrophobic in nature, they are poorly water-soluble and apt to aggregate under physiological condition. Nanoparticle-based delivery vehicles have been introduced to solve these problems.^{11–15} Numerous delivery approaches have been devoted to keep the photosensitizer stable on the carrier in monomeric form, without loss or alteration of its spectroscopic and functional properties.^{16,17}

Upconversion is an anti-Stokes process in which long wavelength radiation, usually near-infrared (NIR) or infrared (IR), is converted to shorter wavelength such as ultraviolet (UV) or visible (VIS) radiation. Upconversion nanoparticles have low toxicity, weak background fluorescence, high detection sensitivity, and deep light-penetration depth in tissues compared with conventional downconversion fluorescent materials.^{18–22} Upon radiation of near-infrared or infrared, upconversion nanoparticles would emit visible light that can be used to excite photosensitizer to generate reactive oxygen species. Modified with photosensitizers, these near-infrared to visible upconversion nanoparticles have the potential of

Received: November 18, 2011

Revised: March 28, 2012

Accepted: April 25, 2012

Published: April 25, 2012

increasing the limited therapeutical depth of current PDT techniques.²³

The application of upconversion nanoparticles in photodynamic therapy has shown promising prospects and attracted much attention. Some groups have shown the potential of photosensitizer modified upconversion nanostructure for near-infrared photodynamic therapy.^{23–27} To our best knowledge, physical encapsulation or physical adsorption was used to keep the photosensitizer close to the upconversion nanocrystal in previous studies. However, the methods of physical adsorption or physical encapsulation by mesoporous silica do not exclude the release of photosensitizer from the nanostructure during systemic circulation, thus leading to phototoxic side effects.^{16,28} To the method of physical encapsulation by silica shell, the efficiency of PDT is low because it is difficult for reactive oxygen species to exit the silica shell for its designed purpose.²⁷

To construct a stable and efficient photosensitized nanodrug, O-carboxymethylated chitosan (OCMC) and chemical covalent linkage were used to modify biofunctional molecules on to upconversion nanoparticles. The choice of O-carboxymethylated chitosan as coating polymer is based on its nontoxicity, biocompatibility, water-solubility and availability for further modification of functional groups.^{29–31} The chitosan coated nanopatform OCMC-UCNP was then comodified with targeting peptide c(RGDyK) and photosensitizer pyropheophorbide a (Ppa) to construct the nanoparticle UCNP-Ppa-RGD. Pyropheophorbide a was chosen as photosensitizer because it has an absorption maximum with high extinction coefficient ($\epsilon_{668\text{nm}} = 4 \times 10^4 \text{ M}^{-1} \text{ cm}^{-1}$) at 668 nm which significantly overlaps with the red emission peak of NaYF₄ nanocrystal. In addition, it has a free carboxylic group for further modification.³² Our objective is to build a highly stable and efficient photosensitizer modified upconversion nanostructure for targeted near-infrared photodynamic therapy of cancer cells.

■ EXPERIMENTAL SECTION

Materials. O-Carboxymethyl chitosan (M_w 200,000, deacetylation degree >60%, substitution degree >60%) was purchased from Aoxing Biochemistry Co. Ltd. (Zhejiang, China). Pyropheophorbide a (Ppa) was purchased from J&K Scientific Ltd. Cyclic Arg-Gly-Asp-(D)-Tyr-Lys c(RGDyK) was purchased from GL Biochem Ltd. (Shanghai, China). CCK8 was purchased from Dojindo Laboratories (Kumamoto, Japan). Fluoresceinyl cypridina luciferin analogue (FCLA) was purchased from Tokyo Kasei Kogyo Co. (Tokyo, Japan). CM-H₂DCFDA, 5-aminofluorescein, N-hydroxysulfosuccinimide (NHS), 1-ethyl-3-(3-(dimethylamino)propyl)-carbodiimide (EDC), di-*tert*-butyl dicarbonate (Boc₂O) and trifluoroacetic acid were purchased from Sigma-Aldrich Co. All chemicals mentioned above were of analytical grade and used without further purification. Deionized water was used throughout.

Polyethylenimine (PEI)-capped NaYF₄:Yb/Er upconversion nanoparticle (PEI-UCNP) was kindly supplied by the Prof. Xianggui Kong research group. It was prepared by solvothermal methods.³³

Synthesis of Upconversion Nanopatform OCMC-UCNP. The upconversion nanopatform OCMC-UCNP was synthesized by wrapping PEI-UCNP nanoparticle with a layer of O-carboxymethyl chitosan. This wrapping process contains two steps. In the first step, amino group of chitosan was protected using boc anhydride and carboxyl group of chitosan

was activated using EDC/NHS. In the second step, PEI-UCNP nanoparticle was wrapped by chitosan utilizing the condensation reaction between the activated carboxyl groups of chitosan and the amino groups of polyethylenimine.

Step 1. O-Carboxymethyl chitosan (10 mg) was dissolved in water (10 mL), di-*tert*-butyl dicarbonate (7.8 mg) was added as a solution in para-dioxane, and the mixture was stirred at room temperature overnight. The reaction mixture was gradually poured into a vigorously stirred solution of ethanol (200 mL). White precipitate was collected by filtration and dried under vacuum. The precipitate was dissolved again in water (10 mL) and activated by EDC/NHS for 2 h (molar ratio, chitosan:EDC:NHS = 1:1:2.5).

Step 2. Nanoparticle PEI-UCNP (10 mg) was added into the final solution of step 1, and the mixture was vortexed for 4 h. The chitosan wrapped nanoparticle OCMC-UCNP was obtained by centrifugation at 10,000 rpm for 10 min and washed three times with deionized water.

Synthesis of UCNP-Ppa-RGD Nanoparticle. UCNP-Ppa-RGD was synthesized in two steps, including the modification of nanopatform OCMC-UCNP first with c(RGDyK), then pyropheophorbide a.

Step 1. c(RGDyK) (1.25 mg) was dissolved in Na₂CO₃ buffer solution (pH 8.0, 2 mL). OCMC-UCNP (5 mg) was added into the solution and vortexed at room temperature for 4 h. The c(RGDyK) modified nanoparticle was isolated by centrifugation and washed as described above.

Step 2. The *t*-Boc-NH group of chitosan was deprotected by dissolving the c(RGDyK) modified nanoparticle in 95% trifluoroacetic acid (2 mL) and stirring gently at room temperature for 2 h. After centrifugation, the precipitation was added into pyropheophorbide a solvent (2 mM, 2 mL), where the photosensitizer had been activated by EDC/NHS for 2 h (molar ratio, Ppa:EDC:NHS = 1:1:2.5). The mixture was stirred for 4 h, and the final product UCNP-RGD-Ppa was isolated by centrifugation and washed as described above.

Characterization. To further examine the morphology and size of the nanoparticles, a JEM-100CXII transmission electron microscope (TEM) with parameters of 100 kV voltage and 70 pA current was used. Samples were prepared by placing a drop of dilute dispersions in water on the surface of copper grids. Fourier transform infrared (FT-IR) spectra were recorded with KBr pellets on a Bio-Rad FTS 6000 spectrometer (Bio-Rad Company, Hercules, CA, USA) at room temperature. The absorption spectra of pyropheophorbide a, OCMC-UCNP and UCNP-RGD-Ppa in water were obtained using a UV/vis spectrometer (Lambda 35, Perkin-Elmer, USA). Fluorescence spectra were obtained using LS-55 fluorescence spectrophotometer (Perkin-Elmer, USA) with an excitation of 414 nm. The upconversion fluorescence spectra of OCMC-UCNP was recorded by using a 150 mW/cm² continuous-wave (CW) 980 nm diode laser as the excitation source. To examine the stability of UCNP-RGD-Ppa, the nanoparticle was soaked in water solution with different pH conditions (pH = 5, 7.4 and 8). Twenty-four hours later, they were centrifuged (10,000 rpm, 10 min) and the supernatants were collected. Fluorescence spectra of the supernatants were measured compared with that of free pyropheophorbide a solution.

Cell Culture. U87-MG human glioblastoma cancer cells (high integrin $\alpha_v\beta_3$ expression) and MCF-7 human breast cancer cells (low integrin $\alpha_v\beta_3$ expression) were cultured in Eagle's minimal essential medium (EMEM) and Dulbecco's modified Eagle's medium (DMEM), respectively. The media

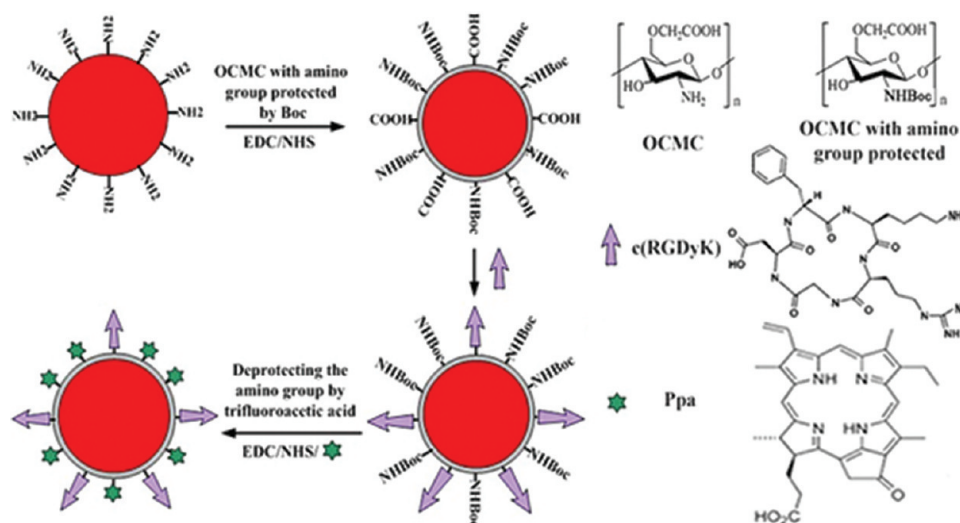


Figure 1. An illustration of the procedures of producing the UCNP-Ppa-RGD nanoparticle.

were supplemented with 10% fetal bovine serum (FBS) and 1% penicillin–streptomycin in 5% CO₂ at 37 °C in a humidified incubator.

Photodynamic Therapy Chemiluminescence of UCNP-RGD-Ppa Mediated by Fluoresceinyl Cypridina Luciferin Analogue (FCLA) in Solution. The basic photodynamic therapy chemiluminescence measurement system is based on measurement of chemiluminescence from fluoresceinyl cypridina luciferin analogue when activated by PDT-generated reactive oxygen species.^{34,35} The experiments were carried out with three parallel groups: (1) 1 μM Ppa and 1 μM FCLA in PBS; (2) 100 μg/mL UCNP-Ppa-RGD (~1 μM pyropheophorbide a) and 1 μM FCLA in PBS; (3) 1 μM FCLA in PBS (control). The total volume of solvent in each group was 1 mL. The prepared samples were transferred to 1 mL glass cuvettes and irradiated with laser (635 nm, 20 mW/cm²). Chemiluminescence signals were collected before and immediately after the laser irradiation.

Targeting Specialty of UCNP-Ppa-RGD to Cancer Cells. To study the integrin targeting specialty of UCNP-Ppa-RGD, both U87-MG and MCF-7 tumor cells were incubated in a serum-free medium containing 100 μg/mL UCNP-Ppa-RGD or 100 μg/mL UCNP-Ppa nanostructures for 30 min and then rinsed with PBS and replaced with fresh cell medium. To further validate that UCNP-Ppa-RGD was internalized into cells mainly through the receptor-mediated endocytosis pathway, preblocking experiments were designed with U87-MG cells' incubation with 2 μM free c(RGDyK) for 30 min before their incubation with UCNP-Ppa-RGD. The cells were imaged by a commercial laser scanning microscope (LSM 510/ConfoCor 2) combination system (Zeiss, Jena, Germany) equipped with a Plan-Neofluar 40×/1.3 NA Oil DIC objective. Pyropheophorbide a was excited at 633 nm, and its fluorescence emission was recorded through a LP650 nm filter.

Intracellular Reactive Oxygen Species Detection. The production of intracellular reactive oxygen species was measured using nonfluorescent compound CM-H₂DCFDA. U87-MG cells were preloaded with 100 μg/mL UCNP-Ppa-RGD and treated with 5 μM CM-H₂DCFDA for 30 min in darkness. Then the cells were irradiated by 980 nm laser (0.5 W/cm²) for different doses of 0, 150, and 300 J/cm², respectively. Production of reactive oxygen species was

visualized by confocal microscope. DCF was excited at 488 nm with an Ar ion laser, and the fluorescence emission was recorded through a 500–550 nm infrared band-pass filter. To quantitatively assess the fluorescence intensity, U87-MG tumor cells were incubated with 100 μg/mL UCNP-Ppa-RGD solution in a 12-well microplate. After similar treatments as mentioned above, cells were washed and resuspended in ice-cold PBS. The fluorescence histograms of cells in different treatments were obtained from 10,000 cells by flow cytometry (Becton Dickinson FACScan).

Selective Photodynamic Therapy of Cancer Cells with UCNP-Ppa-RGD upon Near-Infrared Irradiation. For cell phototherapy studies, U87-MG cells and MCF-7 cells (1 × 10⁴ per well) growing in 35 mm Petri dishes were incubated with UCNP-Ppa or UCNP-Ppa-RGD nanoparticle solution for 30 min. Both solutions were at a concentration of 100 μg/mL. They were then rinsed with PBS and exposed to a 980 nm laser at a fluence of 0.5 W/cm² for 5 min. After being cultured for another 2 h, cancer cells under different treatments were observed using optical microscope.

For CCK8 assay, U87-MG and MCF-7 cancer cells were collected and diluted to a cell density of 1 × 10⁵ /mL in complete medium, and then seeded into 96-well plates (100 mL/well). After being cultured for 24 h, UCNP-Ppa-RGD with different concentrations of 0, 50, 100, 200 μg/mL were added and the cells were incubated for another 24 h at 37 °C. Then the cells were washed to remove the unbound nanoparticle and exposed to 980 nm laser with an output power of 0.5 W/cm² for different doses of 0, 75, 150, 225, 300 J/cm². After incubation at 37 °C for 48 h, cell cytotoxicity was assessed with CCK8. OD450, the absorbance value at 450 nm, was read with a 96-well plate reader (INFINITE M200, Tecan, Switzerland), to determine the cell viability. The cell viability was calculated as follows: cell viability (% of control) = OD_{Tre}/OD_{Con} × 100% (where OD_{Tre} is the absorbance value of treated cells; OD_{Con} is the absorbance value of untreated cells which were exposed to 980 nm laser without treatment with UCNP-Ppa-RGD).

RESULTS

Characteristics of Chitosan-Wrapped Upconversion Nanoparticle OCMC-UCNP. In this work, a photosensitizer

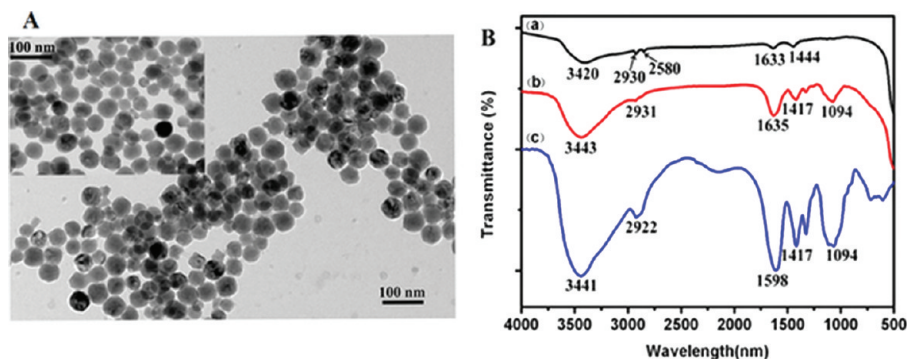


Figure 2. (A) TEM image of OCMC-UCNP. Inset: TEM image of PEI-UCNP. (B) FTIR spectra of PEI-UCNP, OCMC and OCMC-UCNP. The TEM images showed that both OCMC-UCNP and PEI-UCNP nanoparticles were spherical, water dispersible. The average diameters of the nanoparticles before and after chitosan wrapping were measured to be about 50 and 53 nm, respectively. The result of FTIR spectra demonstrated that the nanoparticle PEI-UCNP was successfully wrapped by *O*-carboxymethyl chitosan.

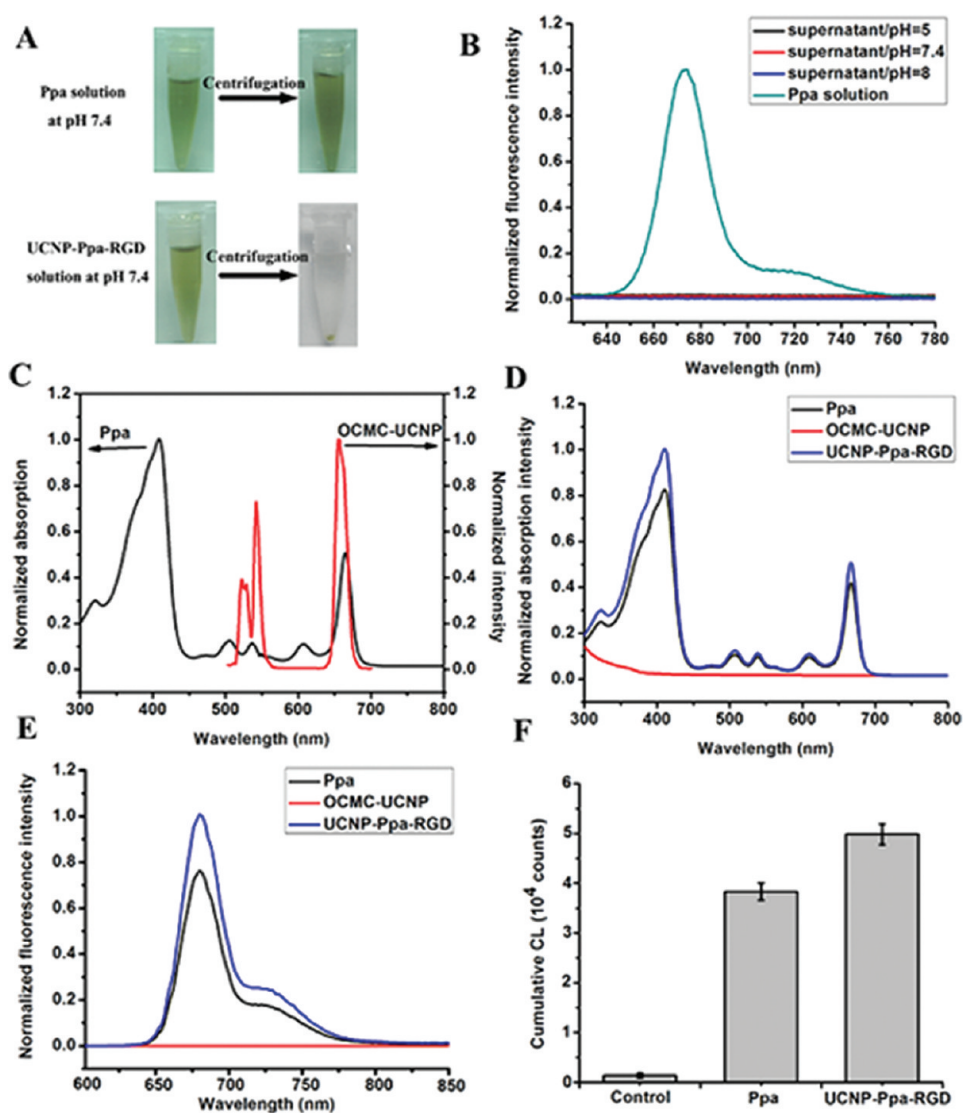


Figure 3. (A) Photos of UCNP-Ppa-RGD and free pyropheophorbide a solutions at pH 7.4; both of the solutions were centrifugated at 10,000 rpm for 10 min. (B) Fluorescence spectra of free pyropheophorbide a solution at pH 7.4 and the supernatants of UCNP-Ppa-RGD solutions under different pH conditions. (C) Absorbance spectrum of pyropheophorbide a and emission spectrum of OCMC-UCNP, $\lambda_{ex} = 980$ nm. (D) Absorbance spectra of pyropheophorbide a, OCMC-UCNP and UCNP-RGD-Ppa in water. (E) Fluorescence spectra of pyropheophorbide a, OCMC-UCNP and UCNP-RGD-Ppa in water. Both of the pyropheophorbide a and UCNP-RGD-Ppa samples have the same photosensitizer concentration of 1 μ M, $\lambda_{ex} = 414$ nm. (F) Comparison of cumulative chemiluminescence in PBS, pyropheophorbide a and UCNP-Ppa-RGD solution, respectively. Both the pyropheophorbide a and UCNP-RGD-Ppa samples have the same photosensitizer concentration, $\lambda_{ex} = 635$ nm.

pyropheophorbide a and RGD peptide c(RGDyK) comodified chitosan-wrapped upconversion nanoparticle UCNP-Ppa-RGD was synthesized. Figure 1 shows the procedures of producing the UCNP-Ppa-RGD nanoparticle. First, polyethylenimine-capped NaYF₄ nanocrystal was wrapped by *O*-carboxymethyl chitosan to develop an upconversion nanoplatform OCMC-UCNP. The nanoplatform was further comodified with c(RGDyK) and pyropheophorbide a to construct the UCNP-Ppa-RGD nanoparticle. *O*-Carboxymethyl chitosan has abundant amino groups and carboxyl groups. The carboxyl groups were used to link with the amino groups of polyethylenimine polymer and targeting peptide, while its amino groups were used to link with the carboxyl groups of photosensitizers.

The absorption spectrum of nanoparticle PEI-UCNP in water was obtained using a UV/vis spectrometer. No characteristic absorption peaks were observed on the absorption spectrum of nanoparticle PEI-UCNP (Figure S1 in the Supporting Information). The Yb ions have a large absorption cross-section around 980 nm and can transfer their energy nonradiatively to the ⁴I_{11/2} erbium level. Thus 980 nm was chosen as the excited wavelength.

The morphology and size of nanoparticle PEI-UCNP and OCMC-UCNP were studied by transmission electron microscope (Figure 2A). Both were spherical and water-dispersible. The average diameters of the nanoparticles before and after chitosan wrapping were measured to be about 50 and 53 nm, respectively. Thus the thickness of the wrapping *O*-carboxymethyl chitosan is approximately 3 nm. FT-IR spectra of PEI-UCNP, OCMC and OCMC-UCNP were measured to demonstrate that chitosan was successfully wrapped upon nanoparticle PEI-UCNP (Figure 2B). Pure *O*-carboxymethyl chitosan shows three strong peaks at 1598, 1417, and 1094 cm⁻¹ (Figure 2B(c)), corresponding to the bending vibration of N-H group, symmetrical stretching vibrations of COO- group and bending vibration of C-O group, respectively. Two peaks on the spectra of PEI-UCNP at 1633 and 1444 cm⁻¹ were assigned to the vibrations of NH₂ group of polyethylenimine (Figure 2B(a)), which is consistent with the report of Wang.³⁶ On the characteristic FT-IR spectrum of OCMC-UCNP, two peaks appear at 1635 and 1094 cm⁻¹ (Figure 2B(b)), ascribed to the -CONH amide band and the C-O bend of *O*-carboxymethyl chitosan, respectively. These results indicate that the nanoparticle PEI-UCNP was successfully wrapped by chitosan through forming the amide linkages between the amino groups of polyethylenimine and the carboxyl groups of chitosan.

Characteristics of UCNP-RGD-Ppa Nanoparticle. The stability of UCNP-RGD-Ppa nanoparticle under different pH conditions was measured. UCNP-RGD-Ppa was soaked in water with different pH of 5, 7.4 and 8, respectively. Twenty-four hours later, the nanoparticle still showed good dispersibility in different pH conditions. After centrifugation, green precipitate and nearly colorless supernatant were observed in all UCNP-RGD-Ppa samples with different pH, while no precipitate or color change was noted in free pyropheophorbide a sample (Figure 3A, the results only show the UCNP-RGD-Ppa samples at pH 7.4). Fluorescence spectra (Figure 3B) also showed that there was no free pyropheophorbide a detected in the supernatants of the nanoparticle samples with different pH. All of these results demonstrate a high stability of UCNP-RGD-Ppa.

Upconversion fluorescence spectra of OCMC-UCNP and absorption spectra of photosensitizer were measured. The

absorption maximum of pyropheophorbide a at 668 nm overlaps significantly with the red emission peak of the NaYF₄ nanocrystal (Figure 3C). The result suggests an efficient energy transfer between the NaYF₄ nanocrystal and the modified photosensitizer.

To check whether the spectroscopic property of photosensitizer had changed after the covalent modification, the absorption and fluorescence spectra of pyropheophorbide a, OCMC-UCNP and UCNP-Ppa-RGD were measured. The absorption spectra (Figure 3D) show UCNP-Ppa-RGD nanoparticle has the same characteristic absorption peaks as pyropheophorbide a does. This indicates that photosensitizer has been successfully conjugated to the nanoplatform without change in its chromophore. Since there are plenty of chemical active groups outside OCMC-UCNP, this nanoplatform has great potential in carrying biofunctional molecules. The loading ability of pyropheophorbide a and c(RGDyK) was measured by the absorbance method, and it was calculated to be 527:2.8:1 upconversion nanoparticle:pyropheophorbide a:c(RGDyK) by weight basis (Figure S2 in the Supporting Information).

By controlling both free pyropheophorbide a and UCNP-Ppa-RGD solvents with equal pyropheophorbide a concentration (1 μM), UCNP-Ppa-RGD exhibits the same fluorescence spectral peak at 678 nm as free pyropheophorbide a does (Figure 3E). However, the fluorescence emission intensity of UCNP-Ppa-RGD is obviously stronger than that of free pyropheophorbide a, probably due to the concentration quenching derived from self-aggregation of pure pyropheophorbide a molecules.

Aggregation of the photosensitizer chromophores can decrease both fluorescence intensity and singlet oxygen generation. To check whether the photosensitizer retained its original functional property, the efficiency of reactive oxygen species generation of both UCNP-Ppa-RGD and free pyropheophorbide a samples was evaluated by fluoresceinyl cypridina luciferin analogue chemiluminescence. The mechanism for photodynamic therapy involves singlet oxygen (¹O₂) generated by energy transfer from photosensitizers. ¹O₂ can react with fluoresceinyl cypridina luciferin analogue, which is a cypridina luciferin analogue and a specific chemiluminescence probe for detecting ¹O₂. The reaction of the probe and ¹O₂ can give emission with peak wavelength at about 532 nm, which can be detected by a highly sensitive intensified charge-coupled device detector.^{34,35} The results (Figure 3F) show the cumulative chemiluminescence of free pyropheophorbide a and UCNP-Ppa-RGD samples. In the result, the cumulative chemiluminescence generated by free pyropheophorbide a is significantly lower than that by UCNP-Ppa-RGD. The decrease in the singlet oxygen generation efficiency is correlated with the decrease in the fluorescence yield because of the low solubility of the photosensitizers and corresponding aggregation effects.

Targeting Specificity of UCNP-Ppa-RGD in Vitro Tumor Cells. Integrin α_vβ₃ plays a pivotal role in tumor angiogenesis and is a receptor for the extracellular matrix proteins with the exposed RGD tripeptide sequence. To demonstrate the α_vβ₃ integrin specificity of the nanoparticle, two different cell lines, U87-MG cells and MCF-7 cells, were used. The results show a strong red fluorescence in U87-MG cells incubated with UCNP-Ppa-RGD, and a low fluorescence both in MCF-7 cells and U87-MG cells incubated with UCNP-Ppa (Figure 4). These results demonstrate that the cyclic pentapeptide c(RGDyK) can selectively bind to α_vβ₃ integrin

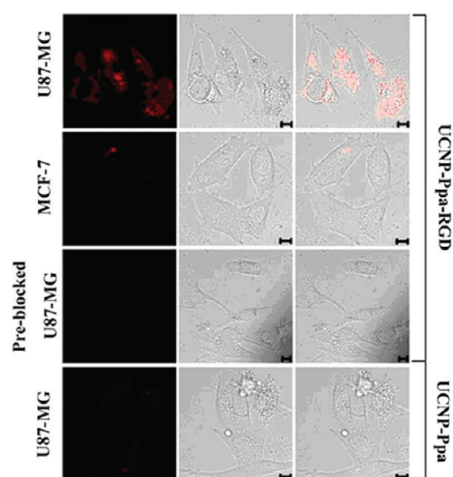


Figure 4. Confocal luminescence images of integrin positive cells (U87-MG) and integrin negative cells (MCF-7) after incubation in a solution of UCNP-RGD-Ppa or UCNP-Ppa under different treatments, $\lambda_{ex} = 488$ nm. Bar scale: 10 μ m.

with high affinity, thus improving the targeting specificity of UCNP-Ppa-RGD to integrin $\alpha_v\beta_3$ -rich tumor cells.

To further validate that UCNP-Ppa-RGD was internalized into cells mainly through the receptor-mediated endocytosis pathway, a preblocking experiment was conducted by incubating U87-MG cells with excess free c(RGDyK) for 30 min before their incubation with UCNP-Ppa-RGD. As a result, significantly lower fluorescence was detected in the c(RGDyK)-treated group than that in the untreated group. This suggests that free RGD peptides blocked the binding of UCNP-Ppa-RGD nanoprobe with $\alpha_v\beta_3$ integrins overexpressed in tumor

cells, accordingly confirming receptor-mediated endocytosis of the nanoparticle to tumor cells.

Dark Toxicity and Phototoxicity of UCNP-Ppa-RGD in Vitro. To demonstrate the biocompatibility of the nanoparticle, we examined the dark cytotoxicity of UCNP-Ppa-RGD on the U87-MG cells using CCK8 assay. U87-MG cells were incubated for 48 h with the UCNP-Ppa-RGD nanoparticle whose concentration ranged from 25 to 400 μ g/mL. The result (Figure 6A) shows the cell viability is still beyond 85% even at 400 μ g/mL dose of UCNP-Ppa-RGD, indicating a low dark cytotoxicity of the nanoparticle.

We evaluated the potential of reactive oxygen species generation caused by UCNP-Ppa-RGD upon 980 nm irradiation in vitro. Photosensitized U87-MG cells were labeled with DCFH-DA for 30 min and imaged after irradiation at 0, 150, 300 J/cm^2 , respectively. The group without irradiation served as control and showed very weak fluorescence, while the other two groups showed a significantly increased fluorescence in cytoplasm where the nanoparticle accumulated (Figure 5A), indicating an intracellular reactive oxygen species generation mediated by UCNP-Ppa-RGD. Such increase was further demonstrated by fluorescence histograms obtained by flow cytometry (Figure 5B). This irradiation dose-dependent cytotoxicity suggests that the UCNP-Ppa-RGD nanoparticle is a promising candidate for near-infrared photodynamic therapy.

Selective Killing of Cancer Cell with UCNP-Ppa-RGD.

Following the PDT treatment, U87-MG and MCF-7 cells were observed using an optical microscope (Figure 6B). Extensive cell death was observed only in U87-MG cells incubated with UCNP-Ppa-RGD, evidenced by drastic cell morphology change (Figure 6B, right column). The cells incubated with UCNP-Ppa showed no significant cell death (Figure 6B, middle column). As control, untreated cells that received light exposure alone remained intact (Figure 6B, left column).

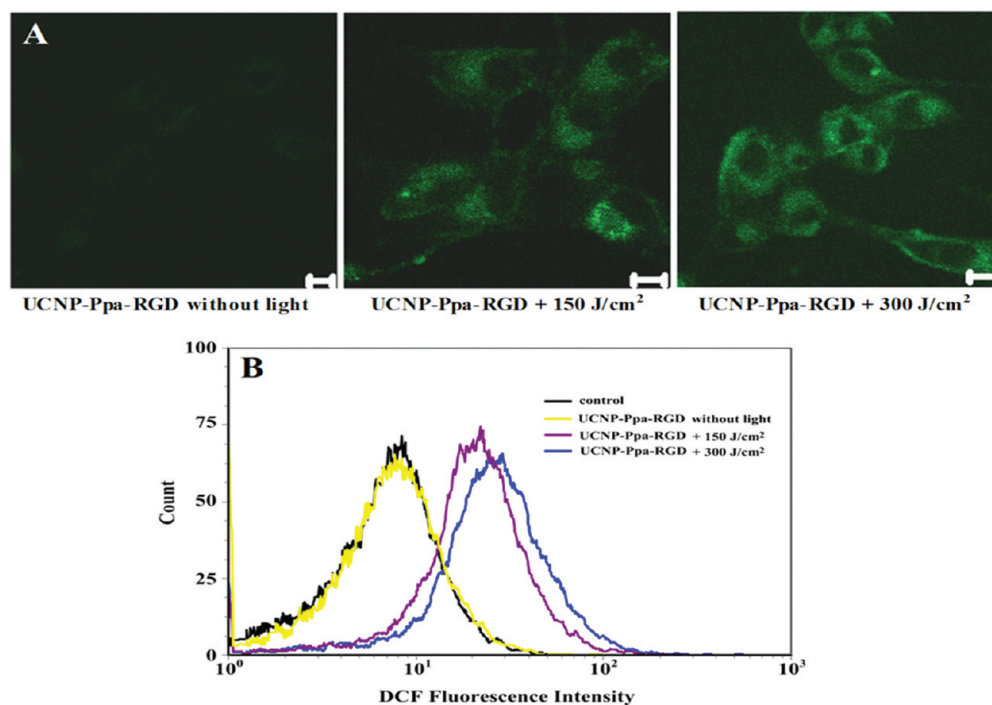


Figure 5. (A) Qualitative characterization of reactive oxygen species generation by DCFH-DA staining using confocal microscopy. (B) Quantitative characterization of reactive oxygen species generation by DCFH-DA staining using flow cytometry. U87-MG cells were incubated with 100 μ g/mL UCNP-Ppa-RGD and 5 μ M of DCFH-DA, and treated with 980 nm laser for different doses of irradiation.

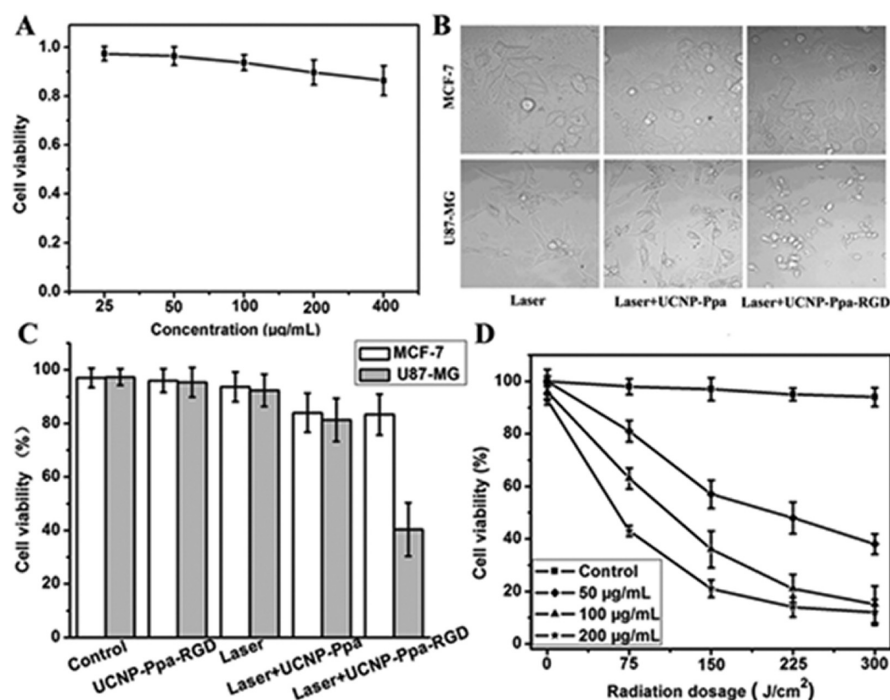


Figure 6. (A) Viability of U87-MG cells after being grown with different concentrations of UCNP-Ppa-RGD for 48 h in the dark. The cell viability still was beyond 85% with high dose of nanoparticle at 400 $\mu\text{g/mL}$. (B) Optical images of U87-MG and MCF-7 cancer cells under different treatments. Extensive cell death was observed only under laser irradiation after tumor cells' incubation with targeting UCNP-Ppa-RGD. (C) Quantification of PDT effect on cancer cell killing under different treatments. Only targeted cancer cells showed an apparent decrease of viability upon irradiation. (D) PDT efficacy vs different concentrations of UCNP-Ppa-RGD and doses of irradiation with 980 nm laser. The control experiment was cells without UCNP-Ppa-RGD under the same radiation dosage. Bars, means \pm SD ($n = 6$).

Under the same experiment conditions, the viability of cells was determined by CCK8. After irradiation, the viability of MCF-7 cells treated by the UCNP-Ppa-RGD nanoparticle showed a negative result, while the viability of U87-MG cancer cells decreased by 30–50% (Figure 6C). Both cells incubated with UCNP-Ppa showed a slight viability decrease of about 8%. No decrease of cell viability was observed when cells were treated by laser irradiation or UCNP-Ppa-RGD nanoparticle alone. These results accord with what was observed under the optical microscope.

To further demonstrate the potential of UCNP-Ppa-RGD in near-infrared photodynamic therapy, U87-MG cells were treated with different concentrations of UCNP-Ppa-RGD together with different doses of photoirradiation. The viability of cells was measured by CCK8 assay (Figure 6D). UCNP-Ppa-RGD with concentrations less than 200 $\mu\text{g/mL}$ exhibited low cytotoxicity before photoirradiation, and the phototoxic effect of UCNP-Ppa-RGD was proportional to the concentration of nanoparticle and the dose of photoirradiation. The optimal PDT-induced cell death could be achieved while the UCNP-Ppa-RGD concentration was higher than 100 $\mu\text{g/mL}$ and the photoirradiation energy was larger than 225 J/cm^2 .

DISCUSSION

For upconversion nanoparticle, stability, monodispersity, biocompatibility and being rich in chemical functional groups are requisite to meet the demand of its bioapplication. Many researchers have focused on the surface chemistry and functional design of upconversion nanoparticles. Several methods such as ligand exchange,³⁷ polymer encapsulation³⁸ and silica coating³⁹ were used to convert the hydrophobic nanocrystals into hydrophilic ones. Although these methods

improved their water solubility, there is still great need to render them with higher biocompatibility and diversity of modification. O-Carboxymethylated chitosan is a derivative of chitosan where the H of hydroxyl group of monomer is replaced by a carboxymethyl group through an ether bond.⁴⁰ It is an ideal polymer in biological applications because it is hydrophilic, biocompatible, nonantigenic and biofunctional.^{29–31} Its amino and carboxyl groups afford the convenience for diverse modification. There is an electrostatic interaction between the positively charged chitosan and the negatively charged cell membrane.⁴¹ In the tumor site, the electrostatic interaction will be enhanced since the acidic microenvironment might increase the positive charges on the surface of chitosan, thereby achieving an effect of tumor-specific accumulation of OCMC-UCNP.^{41,42} When conjugated with targeting or therapeutic or imaging agents, this nanoplatform could become a targeted multifunctional probe for cancer diagnosis or treatment.

Most photosensitizers are poorly water-soluble and aggregate easily under physiological conditions. This aggregation will decrease their quantum yields due to self-quenching, thus affecting their spectroscopic and functional properties.⁴³ For delivery of these drugs, special formulations are required to make them well dispersed into aqueous systems, often by means of nanoparticle-based delivery vehicles.^{11–15} In this work, pyropheophorbide a was modified on to OCMC-UCNP nanoplatform for near-infrared PDT. The fluorescence intensity and singlet oxygen generation produced by free pyropheophorbide a are significantly lower than those produced by UCNP-Ppa-RGD at the same pyropheophorbide a concentration (Figure 3E and 3F). These results indicate that the tested nanoplatform can weaken the concentration dependent

self-aggregation of photosensitizer. The reason is probably that the water solubility of nanoplateform together with the uniform distribution of photosensitizer upon the nanoplateform improved the water dispersibility of pyropheophorbide a.

Stable and targeted drug delivery is a main requirement for PDT. It can increase the concentration of photosensitizer in the site of disease, thus improving efficacy of PDT and reducing side effects.^{10,16,17} To construct a highly stable UCNP-photosensitizer formulation, photosensitizer pyropheophorbide a was modified on to upconversion nanoplateform through covalent linkage. The obtained UCNP-Ppa-RGD nanoparticle exhibits good dispersibility and stability in water solution with different pH conditions (Figure 3A,B). This modified pyropheophorbide a molecule retains its original spectroscopic and functional properties, indicating there is no change in the chromophore.

Integrin $\alpha_v\beta_3$, an important biomarker overexpressed in sprouting tumor vessels and most tumor cells, but not in quiescent endothelium and normal tissues, plays a critical role in tumor angiogenesis and metastasis.⁴⁴ c(RGDyK) peptide can selectively bind to the $\alpha_v\beta_3$ integrin with high affinity, and has been widely used for tumor cell targeting.^{45,46} Here, it was selected as the targeting molecule for targeted near-infrared PDT. Our results exhibit that c(RGDyK) markedly enhances the tumor targeting specificity of the upconversion nanoparticle (Figure 4). The prepared UCNP-Ppa-RGD nanoparticle can specifically target and destroy integrin $\alpha_v\beta_3$ positive tumor cells under near-infrared laser irradiation (Figure 6).

Strong targeting specificity of UCNP-Ppa-RGD is likely due to the joint efforts of an active targeting based on c(RGDyK), a passive targeting based on EPR effects and the electrostatic interaction between chitosan and tumor cell membrane. This electrostatic interaction is helpful to get the nanoparticle to approach the tumor cell membrane and facilitate the binding between RGD peptide and the $\alpha_v\beta_3$ integrin on the surface of the tumor cell. Upon systemic administration, the targeting UCNP-Ppa-RGD nanoparticle could bind with the $\alpha_v\beta_3$ integrin on the surface of melanoma cells and inner walls of tumor vessels, and enter into cytoplasm via receptor-mediated endocytosis pathway.⁴⁶ Upon near-infrared laser irradiation, UCNP-Ppa-RGD could generate reactive oxygen species, causing direct tumor cytotoxicity and vascular damage.⁴⁷ This renders UCNP-Ppa-RGD a great potential for melanoma targeting and selective photodynamic therapy.

There is an efficient energy transfer between the upconversion nanocrystal and the modified photosensitizer because the absorption maximum of pyropheophorbide a overlaps with the red emission peak of the NaYF₄ nanocrystal (Figure 3C). The modified pyropheophorbide a molecule retains its original spectroscopic and functional properties and is not easy to get self-aggregated. Also, it is important to note that the loading ability of pyropheophorbide a in our study (~0.5% (w/w)) is higher than that by physical encapsulation utilizing mesoporous silica (0.1% (w/w)).²⁷ Because of these properties, the UCNP-Ppa-RGD nanoparticle is expected to be efficient in single oxygen generation upon 980 nm laser irradiation. This supposition is confirmed by the experimental results (Figure 5). The nanodrug shows a phototoxic effect which is proportional to its concentration and the dose of photoirradiation. And it is also demonstrated to be effective in destroying tumor cell upon near-infrared laser irradiation (Figure 6).

In vivo toxicity of upconversion nanoparticle has been studied by Xiong et al.⁴⁸ and Chatterjee et al.⁴⁹ The results indicated that mice intravenously injected with 15 mg/kg upconversion nanoparticles survived for 115 days without any evident (observational, histological, hematological and biochemical) toxic effects.⁴⁹ After intravenous injection, the nanoparticles had a rapid accumulation in lungs and spleen, with the highest concentration in the spleen, by about 24 h postinjection. Then the concentration reduced in the liver and spleen, and almost no upconversion luminescence signal was detected in the liver and spleen at 14 days postinjection. However, the presence of upconversion luminescence signals in the intestinal tract indicates a clearance of upconversion nanoparticles via hepatobiliary transport.^{48,49}

One of the main advantages for upconversion nanoparticle based PDT is that it has a deep therapeutical depth. In vivo demonstration of the therapeutical depth, therapeutical efficacy and targeting specificity of UCNP-Ppa-RGD is ongoing research. A “see and treat” approach could be used in vivo by utilizing the UCNP-Ppa-RGD nanoparticle as a single agent for both imaging and therapy.

CONCLUSION

We have reported a highly stable and efficient nanoparticle UCNP-Ppa-RGD for targeted near-infrared photodynamic therapy. Upconversion nanocrystal NaYF₄:Yb/Er was wrapped by O-carboxymethylated chitosan and comodified by pyropheophorbide a (Ppa) and RGD peptide c(RGDyK) to afford the final nanoparticle UCNP-Ppa-RGD. The nanoparticle has improved water solubility, stability, biocompatibility and resistance to photosensitizers' self-aggregation during delivery. It can specifically target integrin $\alpha_v\beta_3$ positive tumor cells and destroy them efficiently under near-infrared laser irradiation. This novel UCNP-Ppa-RGD nanostructure shows great potential for targeted near-infrared photodynamic therapy.

ASSOCIATED CONTENT

Supporting Information

Figure S1, Figure S2 and additional experimental details. This material is available free of charge via the Internet at <http://pubs.acs.org>.

AUTHOR INFORMATION

Corresponding Author

*South China Normal University, MOE Key Laboratory of Laser Life Science, Institute of Laser Life Science, Guangzhou 510631, China. Tel: (+86-20) 8521-0089. Fax: (+86-20) 8521-6052. E-mail: xingda@scnu.edu.cn.

Notes

The authors declare no competing financial interest.

ACKNOWLEDGMENTS

This research is supported by the National Basic Research Program of China (2011CB910402; 2010CB732602), the Program for Changjiang Scholars and Innovative Research Team in University (IRT0829), and the National Natural Science Foundation of China (81101741). The authors thank Dr. Xianggui Kong Key Laboratory of Excited State Process, Changchun Institute of Optics, Fine Mechanics and Physics, Chinese Academy of Sciences, Changchun, China, for providing upconversion nanoparticles.

■ REFERENCES

- (1) Dougherty, T. Photosensitizers: therapy and detection of malignant tumors. *J. Photochem. Photobiol.* **1987**, *45*, 879–889.
- (2) Dougherty, T. J.; Gomer, C. J.; Henderson, B. W.; Jori, G.; Kessel, D.; Korbelik, M.; Moan, J.; Peng, Q. Photodynamic Therapy: Review. *J. Natl. Cancer Inst.* **1998**, *90*, 889–902.
- (3) Moghissi, K.; Dixon, K. Photodynamic therapy (PDT) in esophageal cancer: a surgical view of its indications based on 14 years experience. *Technol. Cancer Res. Treat.* **2003**, *2*, 319–326.
- (4) Canti, G.; Lattuada, D.; Morellia, S.; Nicoiina, A.; Cubeddub, R.; Taronib, P.; Valentini, G. Efficacy of photodynamic therapy against doxorubicin-resistant murine tumors. *Cancer Lett.* **1995**, *93*, 255–259.
- (5) Weishaupt, K. P.; Gomer, C. J.; Dougherty, T. J. Identification of singlet oxygen as the cytotoxic agent in photodestruction of a murine tumor. *Cancer Res.* **1976**, *36*, 2326–2329.
- (6) Frangioni, J. V. In vivo near-infrared fluorescence imaging. *Curr. Opin. Chem. Biol.* **2003**, *7*, 626–634.
- (7) Maeda, H.; Wu, J.; Sawa, T.; Matsumura, Y.; Hori, K. Tumor vascular permeability and the EPR effect in macromolecular therapeutics: a review. *J. Controlled Release* **2000**, *65*, 271–284.
- (8) Brannon-Peppas, L.; Blanchette, J. O. Nanoparticle and targeted systems for cancer therapy. *Adv. Drug Delivery Rev.* **2004**, *56*, 1649–1659.
- (9) Allen, T. M.; Cullis, P. R. Drug delivery systems: entering the mainstream. *Science* **2004**, *303*, 1818–1822.
- (10) Chen, B.; Pogue, B. W.; Hoopes, P. J.; Hasan, T. Vascular and cellular targeting for photodynamic therapy. *Crit. Rev. Eukaryotic Gene Expression* **2006**, *16*, 279–305.
- (11) Konan, Y. N.; Grunly, R.; Allemann, E. State of the art in the delivery of photosensitizers for photodynamic therapy. *J. Photochem. Photobiol., B* **2002**, *66*, 89–106.
- (12) Taillefer, J.; Jones, M. C.; Brasseur, N.; Van Lier, J. E.; Leroux, J. C. Preparation and characterization of pH-responsive polymeric micelles for the delivery of photosensitizing anticancer drugs. *J. Pharm. Sci.* **2000**, *89*, 52–62.
- (13) Van Nostrum, C. F. Polymeric micelles to deliver photosensitizers for photodynamic therapy. *Adv. Drug Delivery Rev.* **2004**, *56*, 9–16.
- (14) Wang, S.; Gao, R.; Zhou, F.; Selke, M. Nanomaterials and singlet oxygen photosensitizers: potential applications in photodynamic therapy. *J. Mater. Chem.* **2004**, *14*, 487–493.
- (15) Gao, D.; Agayan, R. R.; Xu, H.; Philbert, M. A.; Kopelman, R. Nanoparticles for two-photon photodynamic therapy in living cells. *Nano Lett.* **2006**, *6*, 2383–2386.
- (16) Ohulchanskyy, T. Y.; Roy, I.; Goswami, L. N.; Chen, Y.; Bergey, E. J.; Pandey, R. K.; Oseroff, A. R.; Prasad, P. N. Organically modified silica nanoparticles with covalently incorporated photosensitizer for photodynamic therapy of cancer. *Nano Lett.* **2007**, *7*, 2835–2842.
- (17) Cheng, S. H.; Lee, C. H.; Yang, C. S.; Tseng, F. G.; Mou, C. Y.; Lo, L. W. Mesoporous silica nanoparticles functionalized with an oxygen-sensing probe for cell photodynamic therapy: potential cancer theranostics. *J. Mater. Chem.* **2009**, *19*, 1252–1257.
- (18) Yi, G. S.; Chow, G. M. Synthesis of hexagonal-phase NaYF₄:Yb,Er and NaYF₄:Yb,Tm nanocrystals with efficient up-conversion fluorescence. *Adv. Funct. Mater.* **2006**, *16*, 2324–2329.
- (19) Mai, H. X.; Zhang, Y. W.; Sun, L. D.; Yan, C. H. Highly efficient multicolor up-conversion emissions and their mechanisms of monodisperse NaYF₄:Yb, Er core and core/shell-structured nanocrystals. *J. Phys. Chem. C* **2007**, *111*, 13721–13729.
- (20) Wang, X.; Li, Y. D. Monodisperse nanocrystals: general synthesis, assembly, and their applications. *Chem. Commun.* **2007**, *28*, 2901–2910.
- (21) Cheng, L.; Yang, K.; Zhang, S.; Shao, M.; Lee, S. T.; Liu, Z. Highly-sensitive multiplexed in vivo imaging using PEGylated upconversion nanoparticles. *Nano Res.* **2010**, *3*, 722–732.
- (22) Waynant, R. W.; Ilev, I. K.; Gannot, I. Mid-infrared laser applications in medicine and biology. *Philos. Trans. R. Soc., A* **2001**, *359*, 635–644.
- (23) Wang, C.; Tao, H.; Cheng, L.; Liu, Z. Near-infrared light induced in vivo photodynamic therapy of cancer based on upconversion nanoparticles. *Biomaterials* **2011**, *32*, 6145–6154.
- (24) Wang, C.; Cheng, L.; Liu, Z. Drug delivery with upconversion nanoparticles for multi-functional targeted cancer cell imaging and therapy. *Biomaterials* **2011**, *32*, 1110–1120.
- (25) Zhang, P.; Steelant, W.; Kumar, M.; Scholfield, M. Versatile photosensitizers for photodynamic therapy at infrared excitation. *J. Am. Chem. Soc.* **2007**, *129*, 4526–4527.
- (26) Ungun, B.; Prud'homme, R. K.; Budijono, S. J.; Shan, J. N.; Lim, S. F.; Ju, Y. G.; Austin, R. Nanofabricated upconversion nanoparticles for photodynamic therapy. *Opt. Express* **2009**, *17*, 80–86.
- (27) Qian, H. S.; Guo, H. C.; Ho, P. C. L.; Mahendran, R.; Zhang, Y. Mesoporous-silica-coated up-conversion fluorescent nanoparticles for photodynamic therapy. *Small* **2009**, *5*, 2285–2290.
- (28) Dillon, J.; Kennedy, J. C.; Pottier, R. H.; Roberts, J. E. In vitro and in vivo protection against phototoxic side effects of photodynamic therapy by radioprotective agents WR-2721 and WR-77913. *Photochem. Photobiol.* **1988**, *48*, 235–238.
- (29) Jiang, G. B.; Quan, D.; Liao, K.; Wang, H. Novel polymer micelles prepared from chitosan grafted hydrophobic palmitoyl groups for drug delivery. *Mol. Pharmacol.* **2006**, *3*, 152–160.
- (30) Yuan, H.; Lu, L. J.; Du, Y. Z.; Hu, F. Q. Stearic acid-g-chitosan polymeric micelle for oral drug delivery and in vivo absorption. *Mol. Pharmaceutics* **2011**, *8*, 2252–2238.
- (31) Chen, Q. T.; Wang, X.; Chen, F. H.; Zhang, Q. B.; Dong, B.; Yang, H.; Liu, G. X.; Zhu, Y. M. Functionalization of upconverted luminescent NaYF₄:Yb/Er nanocrystals by folic acid–chitosan conjugates for targeted lung cancer cell imaging. *J. Mater. Chem.* **2011**, *21*, 7661–7667.
- (32) Rancan, F.; Helmreich, M.; Molich, A.; Ermilov, E. A.; Jux, N.; Roder, B.; Hirsch, A.; Bohm, F. Synthesis and in Vitro Testing of a Pyropheophorbide-a-Fullerene Hexakis Adduct Immunoconjugate for Photodynamic Therapy. *Bioconjugate Chem.* **2007**, *18*, 1078–1086.
- (33) Wang, F.; Fan, X. P.; Wang, M. Q.; Zhang, Y. Multicolour PEI/NaGdF₄:Ce³⁺, Ln³⁺ nanocrystals by single-wavelength excitation. *Nanotechnology* **2007**, *18*, 025701.
- (34) Wei, Y. C.; Zhou, J.; Xing, D. In vivo monitoring of singlet oxygen using delayed chemiluminescence during photodynamic therapy. *J. Biomed. Opt.* **2007**, *12* (1), 014002.
- (35) Wang, J.; Xing, D.; He, Y. H.; Hu, X. J. Experimental study on photodynamic diagnosis of cancer mediated by chemiluminescence probe. *FEBS Lett.* **2002**, *523*, 128–132.
- (36) Wang, F.; Chatterjee, D. K.; Li, Z.; Zhang, Y.; Fan, X.; Wang, M. Synthesis of polyethylenimine/NaYF₄ nanoparticles with upconversion fluorescence. *Nanotechnology* **2006**, *17*, 5786–5791.
- (37) Zhang, T. R.; Ge, J. P.; Hu, Y. X.; Yin, Y. D. A General Approach for Transferring Hydrophobic Nanocrystals into Water. *Nano Lett.* **2007**, *7*, 3203–3207.
- (38) Lin, C. A.; Sperling, R. A.; Li, J. K.; Yang, T. Y.; Li, P. Y.; Zanella, M.; Chang, W. H.; Parak, W. J. Design of an Amphiphilic Polymer for Nanoparticle Coating and Functionalization. *Small* **2008**, *4*, 334–341.
- (39) Yang, J. P.; Deng, Y. H.; Wu, Q. L.; Zhou, J.; Bao, H. F.; Li, Q.; Zhang, F.; Li, F. Y.; Tu, B.; Zhao, D. Y. Mesoporous Silica Encapsulating Upconversion Luminescence Rare-Earth Fluoride Nanorods for Secondary Excitation. *Langmuir* **2010**, *26*, 8850–8856.
- (40) Kim, K. W.; Thomas, R. L.; Lee, C.; Park, H. J. Antimicrobial activity of native, degraded and O-carboxymethylated chitosan. *J. Food Prot.* **2003**, *66*, 1495–1498.
- (41) Yang, R.; Shim, W. S.; Cui, F. D.; Cheng, G.; Han, X.; Jin, Q. R.; Kim, D. D.; Chung, S. J.; Shim, C. K. Enhanced electrostatic interaction between chitosan-modified PLGA nanoparticle and tumor. *Int. J. Pharm.* **2009**, *371*, 142–147.
- (42) Schmitt-Sody, M.; Strieth, S.; Krasnici, S.; Sauer, B.; Schulze, B.; Teifel, M.; Michaelis, U.; Naujoks, K.; Dellian, M. Neovascular targeting therapy: paclitaxel encapsulated in cationic liposomes improves antitumoral efficacy. *Clin. Cancer Res.* **2003**, *9*, 2335–2341.

(43) Kirchherr, A. K.; Briel, A.; Mader, K. Stabilization of indocyanine green by encapsulation within micellar systems. *Mol. Pharmaceutics* **2009**, *6*, 480–491.

(44) Hood, J. D.; Cheres, D. A. Role of integrins in cell invasion and migration. *Nat. Rev. Cancer* **2002**, *2*, 91–100.

(45) Pierschbacher, M.; Ruoslahti, E. Cell attachment activity of fibronectin can be duplicated by small synthetic fragments of the molecule. *Nature* **1984**, *309*, 30–33.

(46) Li, Z. M.; Huang, Peng.; Zhang, X. J.; Lin, J.; Yang, S.; Liu, B.; Gao, F.; Xi, P.; Ren, Q. S.; Cui, D. X. RGD-conjugated dendrimermodified gold nanorods for in vivo tumor targeting and photothermal therapy. *Mol. Pharmaceutics* **2009**, *7*, 94–104.

(47) Verma, S.; Watt, G. M.; Mai, Z. M.; Hasan, T. Strategies for Enhanced Photodynamic Therapy Effects. *Photochem. Photobiol.* **2007**, *83*, 996–1005.

(48) Xiong, L. Q.; Yang, T. S.; Yang, Y.; Xu, C. J.; Li, F. Y. Long-term in vivo biodistribution imaging and toxicity of polyacrylic acid-coated upconversion nanophosphors. *Biomaterials* **2010**, *31*, 7078–7085.

(49) Chatterjee, D. K.; Rufaihaha, A. J.; Zhang, Y. Upconversion fluorescence imaging of cells and small animals using lanthanide doped nanocrystals. *Biomaterials* **2008**, *29*, 937–943.